

## ARTICLES

Fluorescence Anisotropy Decay and Solvation Dynamics in a Nanocavity: Coumarin 153 in Methyl  $\beta$ -Cyclodextrins

Pratik Sen, Durba Roy, Sudip Kumar Mondal, Kalyanasis Sahu, Subhadip Ghosh, and Kankan Bhattacharyya\*

Physical Chemistry Department, Indian Association for the Cultivation of Science, Jadavpur, Kolkata 700 032, India

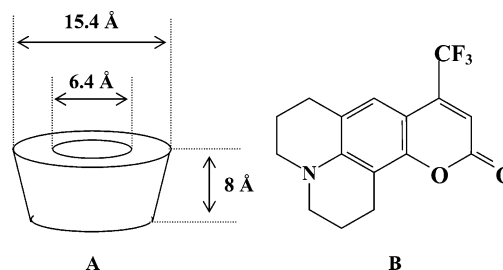
Received: March 30, 2005; In Final Form: June 3, 2005

Fluorescence anisotropy decay and solvation dynamics of coumarin 153 (C153) are studied in dimethyl  $\beta$ -cyclodextrin (DIMEB) and trimethyl  $\beta$ -cyclodextrin (TRIMEB) nanocavity in water. C153 binds to DIMEB and TRIMEB to form both 1:1 and 1:2 (C153:cyclodextrin) complexes. The anisotropy decays of C153 in DIMEB and TRIMEB are found to be biexponential. The fast component of anisotropy decay ( $\sim 1000$  ps) is attributed to the 1:1 complex and the slower one ( $\sim 2500$  ps) to the 1:2 complex. From the components of the anisotropy decay, the length of the 1:1 and 1:2 complexes are estimated. Solvation dynamics of C153 in DIMEB exhibits a very fast (2.4 ps) component (41%) and two slower components of 50 ps (29%) and 1450 ps (30%). Solvation dynamics in TRIMEB is described by three slow components of 10.3 ps (24%), 240 ps (45%), and 2450 ps (31%). Possible origins of the ultraslow components are discussed.

## 1. Introduction

Dynamics in a confined environment is a subject of very active recent interest because of its implications in structure and function of biological assemblies. A supramolecule consisting of a cyclodextrin (CD) as a host with an organic guest molecule encapsulated inside the cavity is an elegant example of a confined system.<sup>1,2</sup> In an aqueous solution, often only a few fluorescent probe (guest) molecules bind to the CD and a very large number of the probe molecules remain in free form in bulk water. Recently, several functionalized CDs (e.g. methyl, hydroxypropyl  $\beta$ -CDs, etc.) have been developed which are much more soluble in water than the unsubstituted CD's.<sup>2</sup> The cavity of the alkyl CDs are more hydrophobic. The higher water solubility of the alkyl CDs ensures solubilization of sparingly soluble organic solutes in water and almost complete binding to the CDs. As a result, alkyl CDs are widely used in drug delivery.<sup>2a</sup> The CDs prevent misfolding and aggregation of proteins by encapsulating the aromatic residues of a protein.<sup>2b</sup> Despite versatile applications of the alkyl CDs in pharmaceutical industry and in biology, photophysics in alkyl CDs has not been explored to a large extent.<sup>1d–e</sup> In this work, we report on anisotropy decay and solvation dynamics of coumarin 153 in two methyl substituted  $\beta$ -CDs, dimethyl  $\beta$ -CD (DIMEB) and trimethyl  $\beta$ -CD (TRIMEB). DIMEB contains only seven hydroxyl groups (one for each glucose unit), while TRIMEB contains no hydroxyl groups.

The rotational dynamics of a fluorescent probe (solute) in a confined medium may be monitored using decay of fluorescence anisotropy. The anisotropy decay is sensitive to the shape and

SCHEME 1: (A)  $\beta$ -Cyclodextrin; (B) Coumarin 153 (C153)

size of the confined environment and is often complicated by the motion of the macromolecules superimposed on the motion of the probe. Many groups have carefully analyzed fluorescence anisotropy decay in DNA,<sup>3a</sup> reverse micelles,<sup>3b</sup> micelles,<sup>3c,d</sup> polymer–surfactant aggregate,<sup>3e</sup> and unsubstituted cyclodextrin.<sup>4b</sup> The size of a  $\beta$ -CD cavity (Scheme 1A) is rather small with an inner diameter  $\sim 6.5$  Å and outer diameter  $\sim 15$  Å.<sup>1b</sup> The height of an unsubstituted  $\beta$ -CD is  $\sim 8$  Å.<sup>1b</sup> The height of a DIMEB (or TRIMEB) cavity is slightly longer ( $\sim 10.9$  Å)<sup>2c</sup> because of the extra methyl groups. According to a MM2 calculation length of the fluorescent probe, coumarin 153 (C153, Scheme 1B) is  $\sim 10$  Å and the width is  $\sim 7$  Å. Thus C153 is expected to fit quite tightly in a  $\beta$ -CD cavity, as suggested by Scypinski and Drake.<sup>4a</sup> There is very little scope of wobbling or translation of the probe (C153) in the  $\beta$ -CD, DIMEB or TRIMEB cavity. Thus the wobbling-in-cone model,<sup>3</sup> commonly used to analyze the anisotropy decay in a micelle and other macromolecular assemblies, may not be applicable to this case. Confinement of a probe inside the CD cavity increases the hydrodynamic diameter of the system (the sum of the lengths of the host, the CD, and the guest), and this causes slowing of the anisotropy

\* To whom correspondence should be addressed. Fax: (91)-33-2473-2805. E-mail: pckb@mahendra.iacs.res.in.

decay. Waldeck and co-workers found that rotational relaxation time of oxazine increases from 125 ps in bulk water to 400 ps inside a  $\beta$ -CD cavity.<sup>4b</sup> In the present work, we show that the hydrodynamic diameter, i.e., length of the 1:1 and 1:2 (probe: CD) complexes, may be determined from the fluorescence anisotropy decay of C153 bound to DIMEB and TRIMEB.

The solvation dynamics of the water molecules in a confined environment may be studied using time-dependent fluorescence Stokes shift. Solvation dynamics in bulk water (and other polar solvents) is ultrafast and occurs in a time scale  $< 1$  ps.<sup>5</sup> However, many organized assemblies exhibit a slow component on a 100–1000 ps time scale.<sup>6–18</sup> This includes cyclodextrin,<sup>7</sup> protein,<sup>8</sup> micelle,<sup>9</sup> reverse micelle,<sup>10</sup> DNA,<sup>11</sup> nanoporous sol-gel glass,<sup>12</sup> lipid,<sup>13</sup> and polymer and polymer surfactant aggregates.<sup>14</sup> To describe the dynamics in a complex and confined assembly in microscopic details, it is necessary to take into account the intermolecular forces and motion of a large number of atoms. Very recently, several groups have carried out large-scale computer simulations of solvation dynamics in proteins,<sup>15</sup> micelle,<sup>16</sup> reverse micelle,<sup>17</sup> and other confined systems and interfaces.<sup>18</sup> Many of these simulations reveal the presence of an ultraslow component ( $> 100$  ps) of solvation dynamics.

Study of the dynamics of water (or other polar solvent) molecules inside a CD cavity are still very few. Fleming and co-workers first reported an ultraslow component of solvation dynamics of  $\sim 1000$  ps in a  $\gamma$ -CD cavity.<sup>7a</sup> Subsequently, Sen et al. detected a slow (nanosecond) component of solvation dynamics of dimethylformamide (DMF) in a  $\beta$ -CD cavity.<sup>7c</sup> In the present work, we compare solvation dynamics of C153 in an aqueous solution of di- and trimethyl  $\beta$ -CDs (DIMEB and TRIMEB). DIMEB contains seven secondary hydroxyl groups which may form hydrogen bonds with water. However, in TRIMEB there are no such hydroxyl groups.

## 2. Experimental Section

Coumarin 153 (C153, Exciton, Scheme 1B), heptakis(2,3,6-tri-*O*-methyl)- $\beta$ -cyclodextrin (TRIMEB, Fluka) and dimethyl- $\beta$ -cyclodextrin (DIMEB, Aldrich) were used as received. The steady-state absorption and emission spectra were recorded in a Shimadzu UV-2401 spectrophotometer and a Spex Fluoro-Max-3 spectrofluorimeter, respectively. Viscosity of the sample solutions was measured using a Ubbelohde viscometer. The fluorescence quantum yield ( $\phi_f$ ) is determined using the reported  $\phi_f$  of C153 in water ( $\phi_f = 0.12$ ).<sup>19</sup> All experiments are carried out at 20 °C.

For picosecond lifetime measurements, the samples were excited at 405 nm using a picosecond diode laser (IBH Nanoled-07) in an IBH Fluorocube apparatus. The emission was collected at a magic angle polarization using a Hamamatsu MCP photomultiplier (5000U-09). The time-correlated single-photon counting (TCSPC) setup consists of an Ortec 9327 CFD and a Tennelec TC 863 TAC. The data are collected with a PCA3 card (Oxford) as a multichannel analyzer. The typical full width at half-maximum (fwhm) of the system response using a liquid scatterer is about 90 ps. The picosecond fluorescence decays were deconvoluted using IBH DAS6 software.

In our femtosecond upconversion setup (FOG 100, CDP) the sample was excited at 405 nm using the second harmonic of a mode-locked Ti-sapphire laser (Tsunami, Spectra Physics) pumped by 5 W Millennia (Spectra Physics). The Tsunami produces 810 nm laser pulses having pulse duration of 50 fs, a repetition rate of 80 MHz, and pulse energy  $\sim 8.5$  nJ. The fundamental 810 nm beam was frequency doubled in a nonlinear

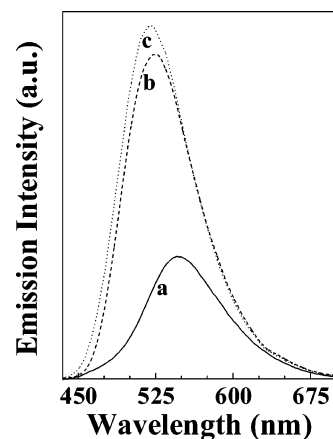


**Figure 1.** Steady-state emission spectra of C153 ( $\lambda_{\text{ex}} = 405$  nm) in (a) water (—), (b) 130 mM DIMEB (---), and (c) 130 mM TRIMEB (···).

crystal (1 mm beta barium borate (BBO),  $\theta = 25^\circ$ ,  $\phi = 90^\circ$ ). The polarization of the second harmonic excitation beam was rotated by a Berek compensator so as to collect the emission decay at magic angle polarization. To avoid possible photo-degradation, the laser power was reduced to  $\sim 40$  mW by placing neutral density filters before the sample, and the sample was placed in a rotating cell of path length 1 mm. The fluorescence emitted from the sample was upconverted in a nonlinear crystal (0.5 mm BBO,  $\theta = 38^\circ$ ,  $\phi = 90^\circ$ ) using a gate beam of 810 nm. The upconverted light is dispersed in a monochromator and detected using photon counting electronics. A cross-correlation function obtained using the Raman scattering from ethanol displayed a fwhm = 350 fs. The femtosecond fluorescence decays were fitted using a Gaussian shape for the exciting pulse.

To study picosecond fluorescence anisotropy decay, the analyzer was rotated at regular intervals to get perpendicular ( $I_{\perp}$ ) and parallel ( $I_{\parallel}$ ) components ( $\lambda_{\text{em}} = 490$  nm). Then the anisotropy function,  $r(t)$ , was calculated using the formula

$$r(t) = \frac{I_{\parallel}(t) - GI_{\perp}(t)}{I_{\parallel}(t) + 2GI_{\perp}(t)} \quad (1)$$

As described by O'Connor and Philips,<sup>20a</sup> at long time, the intensity of the emitted light with parallel and perpendicular polarization should be equal so that  $r(t)$  (described in eq 1) is zero. This is known as the tail matching method and was used to determine the  $G$  value of our picosecond setup. In this method, one uses a probe whose rotational relaxation time ( $\tau_R$ ) is very short compared to the lifetime ( $\tau_f$ ) of the probe.<sup>20a</sup> We used coumarin 153 in methanol for which it is reported that  $\tau_R = 35$  ps<sup>20b</sup> and  $\tau_f = 4200$  ps;<sup>20c</sup> i.e.,  $\tau_R \ll \tau_f$ . Following this method, the  $G$  value of our picosecond setup is found to be 1.8.

## 3. Results

**3.1. Steady-State Emission Spectra.** In an aqueous solution, C153 exhibits emission maximum at 549 nm with emission quantum yield ( $\phi_f$ ) of 0.12.<sup>19</sup> The steady-state emission spectra of C153 in an aqueous solution containing DIMEB and TRIMEB are given in Figure 1. In an aqueous solution, on addition of DIMEB and TRIMEB, the emission maximum of C153 shifts to 525 nm ( $\phi_f = 0.29$ ) in 130 mM DIMEB and to 520 nm ( $\phi_f = 0.33$ ) in 130 mM TRIMEB. The larger blue shift

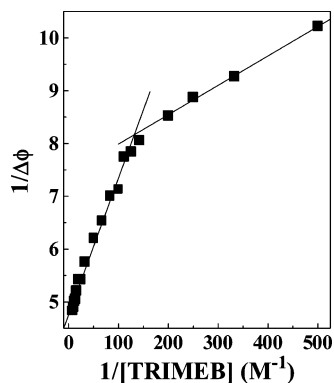
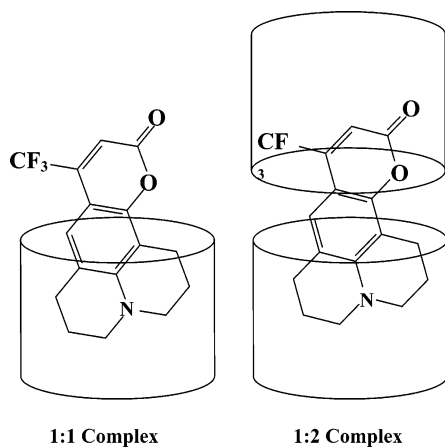


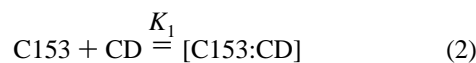
**Figure 2.** Plot of  $1/\Delta\phi$  vs  $1/[\text{TRIMEB}]$  for C153 in water.

### SCHEME 2: 1:1 and 1:2 Complexes of C153 with Methyl $\beta$ -Cyclodextrin



in TRIMEB indicates lower polarity and a more hydrophobic nature of the TRIMEB cavity which has no hydroxyl group.

In an earlier study, Scypinski and Drake<sup>4a</sup> reported formation of a 1:1 complex between C153 and unsubstituted  $\beta$ -CD with a binding constant of  $54 \text{ M}^{-1}$ . In the present work, the binding equilibria of C153 to DIMEB and TRIMEB were analyzed in terms of both 1:1 and 1:2 (C153:CD) complexes (Scheme 2). The 1:1 complex corresponds to the following equilibrium,



At lower CD concentrations ( $<10 \text{ mM}$ ), where the contribution of the 1:2 complex is small, the value of  $K_1$  may be determined from the double reciprocal plot of the change in the emission quantum yield ( $\Delta\phi$ ) against the CD concentration (Figure 2), as described by Hoshino et al.<sup>21</sup> For 1:1 (C153:CD) complexes the value of  $K_1$  is determined to be 220 and  $1220 \text{ M}^{-1}$  for DIMEB and TRIMEB, respectively (Figure 2 and Table 1).

At higher CD concentration, the double reciprocal plot (Figure 2) exhibits a distinct change in slope, presumably because of

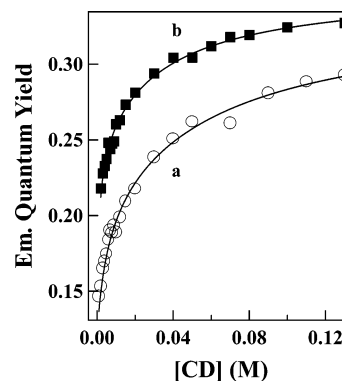
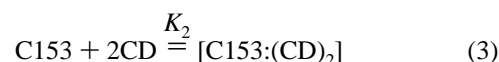


**Figure 3.** Plot of emission quantum yield ( $\phi$ ) of C153 vs  $[\text{CD}]$  in water with varying concentrations of the CDs (a) DIMEB ( $\circ$ ) and (b) TRIMEB ( $\blacksquare$ ). The points represent experimental values, and the solid line represents the nonlinear least-squares fit corresponding to eq 4.

the formation of 1:2 complexes. The 1:2 complex corresponds to the following equilibrium,



If  $\phi_0$ ,  $\phi_1$ , and  $\phi_2$  denote emission quantum yields of the free, 1:1, and 1:2 complexes, the observed emission quantum yield  $\phi$  is given by

$$\phi = \frac{\phi_0 + \phi_1 K_1 [\text{CD}] + \phi_2 K_2 [\text{CD}]^2}{1 + K_1 [\text{CD}] + K_2 [\text{CD}]^2} \quad (4)$$

The values of  $\phi_1$ ,  $\phi_2$ , and  $K_2$  were obtained by a nonlinear least-squares fitting of  $\phi_f$  against  $[\text{CD}]$  as shown in Figure 3. For 1:2 (C153:CD) complexes the value of  $K_2$  is determined to be  $3350$  and  $38500 \text{ M}^{-2}$  for DIMEB and TRIMEB, respectively (Table 1).

The contribution of the probe (C153) in free, 1:1, and 1:2 complexes may be calculated for a particular concentration of CD. If  $C$ ,  $C_0$ ,  $C_1$ , and  $C_2$  represent the concentrations of the probe (C153) in total, free, 1:1, and 1:2 complexes, respectively, then

$$C_0 = \frac{C}{1 + K_1 [\text{CD}] + K_2 [\text{CD}]^2} \quad (5)$$

$$C_1 = K_1 C_0 [\text{CD}] \quad (6)$$

$$C_2 = K_2 C_0 [\text{CD}]^2 \quad (7)$$

From this it is readily calculated that, in a  $130 \text{ mM}$  DIMEB solution, 66% of the probe C153 are bound to DIMEB in the form of a 1:2 complex and 33% as a 1:1 complex and only 1% remains free. For  $130 \text{ mM}$  TRIMEB, 80.3% of C153 is present as the 1:2 complex and 19.6% as the 1:1 complex and only 0.1% remains in the free form. The results are tabulated in Table 1. In summary, in a substituted  $\beta$ -CD a vast majority of the

**TABLE 1: Binding Constant, Emission Quantum Yield, and Relative Contributions of 1:1 and 1:2 Complexes for C153 in 130 mM DIMEB and TRIMEB**

	C153–DIMEB	C153–TRIMEB		C153–DIMEB	C153–TRIMEB
$K_1^a$ ( $\text{M}^{-1}$ )	220	1220	amt of probe in 1:2 complex <sup>a</sup> (%)	66	80.3
$K_2^a$ ( $\text{M}^{-2}$ )	3350	38500	$\phi_1^a$	0.23	0.26
amt of free probe <sup>a</sup> (%)	1	0.1	$\phi_2^a$	0.33	0.35
amt of probe in 1:1 complex <sup>a</sup> (%)	33	19.6			

<sup>a</sup>  $\pm 10\%$ .

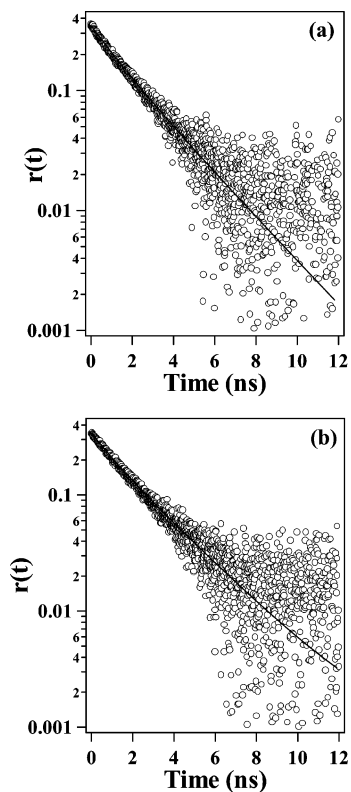


**Figure 4.** (a) Fluorescence anisotropy decay of C153 along with the fitted curve in 130 mM DIMEB in water at 490 nm ( $\lambda_{\text{ex}} = 405$  nm). (b) Fluorescence anisotropy decay of C153 along with the fitted curve in 130 mM TRIMEB in water at 490 nm ( $\lambda_{\text{ex}} = 405$  nm).

probe (C153) molecules exists as the 1:2 complex, a relatively fewer number as the 1:1 complex and only very few C153 molecules remain in free form.

In a saturated (16.3 mM<sup>1b</sup>) aqueous solution of unsubstituted  $\beta$ -CD, according to the reported<sup>4a</sup> binding constant of  $54 \text{ M}^{-1}$  only 47% C153 remains bound to the unsubstituted  $\beta$ -CD. The binding constants of C153 to DIMEB and TRIMEB are larger than that with the unsubstituted  $\beta$ -CD. This and the higher solubility of DIMEB and TRIMEB in water lead to almost complete (>99%) binding of C153 to DIMEB and TRIMEB.

In the following sections, we will first analyze the anisotropy decay of the 1:1 and 1:2 complexes. Finally, we describe solvation dynamics in these systems.

**3.3. Fluorescence Anisotropy Decay.** The fluorescence anisotropy decays of C153 in an aqueous solution containing 130 mM methyl-substituted cyclodextrins (DIMEB and TRIMEB) are shown in Figure 4a,b. The very high initial anisotropy (0.35 and 0.34) suggests that a picosecond setup captures almost the entire rotational dynamics in this case. Obviously, both the 1:1 and 1:2 complexes contribute to the anisotropy decay, and the overall decay is biexponential. The faster of the two decay components are ascribed to the 1:1 complex and the slower to the 1:2 complex. The anisotropy decay data were fitted to two exponentials with amplitudes the same as the relative contribution of the 1:1 and 1:2 complexes as obtained from steady-

state emission measurements (Table 1). The faster component of anisotropy decay is 1150 ps for DIMEB (1000 ps for TRIMEB). The slower component is 2700 ps for DIMEB and 2500 ps for TRIMEB (Table 2). The anisotropy decay of C153 in DIMEB and TRIMEB is markedly slower than that in bulk water ( $\tau_{\text{R}} \sim 100 \text{ ps}^{\text{9d}}$ ). The slower anisotropy decay, a marked blue shift of the emission maximum and an  $\sim 3$ -fold increase in  $\phi_{\text{f}}$  of C153 in DIMEB and TRIMEB compared to those in water, suggests that the probe is trapped inside the cavity of DIMEB and TRIMEB. A simple MM2 calculation also indicates that C153 is partially included in DIMEB and TRIMEB.

The time constant of anisotropy decay ( $\tau_{\text{R}}$ ) is related to the hydrodynamic radius ( $r_{\text{h}}$ ) as<sup>3</sup>

$$\tau_{\text{R}} = \frac{4\pi\eta r_{\text{h}}^3}{3KT} \quad (8)$$

Using the measured viscosity of 130 mM DIMEB in water at 20 °C ( $\sim 1.7 \text{ mPa s}$ ) and the faster component of anisotropy decay, the hydrodynamic radius for the 1:1 complex is estimated to be  $8.7 \pm 0.5 \text{ \AA}$  for 1:1 complex for DIMEB (Table 2). This corresponds to a diameter of  $\sim 17.4 \text{ \AA}$ . This is larger than the reported height (10.9  $\text{\AA}$ ) for DIMEB.<sup>2c</sup> This suggests that in the 1:1 complex a part of the probe is projected out of the cavity so that the length of the system (C153:DIMEB) is larger than that of the DIMEB cavity. For TRIMEB, according to anisotropy studies, the hydrodynamic radius for the 1:1 complex is  $8.3 \pm 0.5 \text{ \AA}$  (Table 2). This suggests a portion of the probe is projected out of the TRIMEB cavity.

To determine the hydrodynamic radius of the 1:2 complex, we used the slower component of anisotropy decay (2700 ps for DIMEB and 2500 ps for TRIMEB). From this the hydrodynamic radii of the 1:2 complex for DIMEB and TRIMEB are  $11.6 \pm 0.5 \text{ \AA}$  and  $11.3 \pm 0.5 \text{ \AA}$ , respectively. This corresponds to a diameter of  $\sim 22 \text{ \AA}$ , which is roughly equal to the sum of the height of two DIMEB (or TRIMEB) cavities.

**3.4. Time-Resolved Studies: Wavelength Dependent Decays.** **3.4.1. Picosecond Result for C153 in DIMEB.** The fluorescence decays of C153 in methyl cyclodextrins were found to be very strongly dependent on the emission wavelengths. In 130 mM DIMEB, at the blue end, 490 nm, the fluorescence decay of C153 is found to be triexponential with three decay components of 100 ps (28%), 1200 ps (19%), and 4700 ps (53%). While at the red end, 600 nm, the decay of time constant 4400 ps is preceded by two distinct rise constants of 300 and 1980 ps, as depicted in Figure 5. Following the procedure of Fleming and Maroncelli,<sup>23a</sup> the time-resolved emission spectra (TRES) were constructed using the parameters of best fit to the fluorescence decays and the steady-state emission intensities.

**3.4.2. Femtosecond Result on C153 in DIMEB.** To detect the ultrafast components of solvation dynamics of C153 bound to DIMEB, we recorded the fluorescence decays using a femtosecond up-conversion setup. In this case, at 490 nm, the fluorescence decay is triexponential with three decay components of 4.5 ps (16%), 59 ps (25%), and 4700 ps (59%). At the red end, 600 nm, the decay of time constant 4400 ps is preceded

**TABLE 2: Parameters of Fluorescence Anisotropy Decay of C153 in 130 mM DIMEB and TRIMEB**

	C153–DIMEB	C153–TRIMEB		C153–DIMEB	C153–TRIMEB
$r_0$	0.35	0.34	$a_{2\text{R}}^a$	0.67	0.80
$r_{\infty}$	0	0	$\tau_{2\text{R}}^a$ (ps)	2700	2500
$a_{1\text{R}}^a$	0.33	0.20	$r_{\text{h}}(1:1)^b$ ( $\text{\AA}$ )	8.7	8.3
$\tau_{1\text{R}}^a$ (ps)	1150	1000	$r_{\text{h}}(1:2)^b$ ( $\text{\AA}$ )	11.6	11.3

<sup>a</sup>  $\pm 10\%$ . <sup>b</sup>  $\pm 0.5 \text{ \AA}$ .

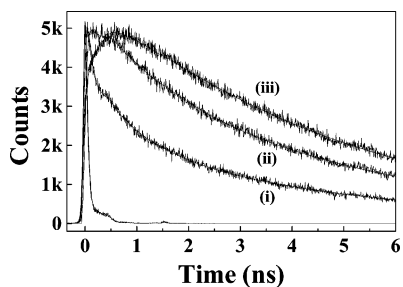


**Figure 5.** Fluorescence decays of C153 in 130 mM DIMEB in water at (i) 455, (ii) 490, and (iii) 600 nm recorded in a picosecond setup.

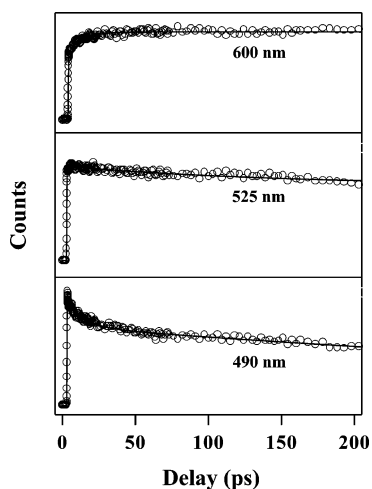


**Figure 6.** Fluorescence decays of C153 in 130 mM DIMEB in water at (i) 490, (ii) 525, and (iii) 600 nm recorded in a femtosecond setup.

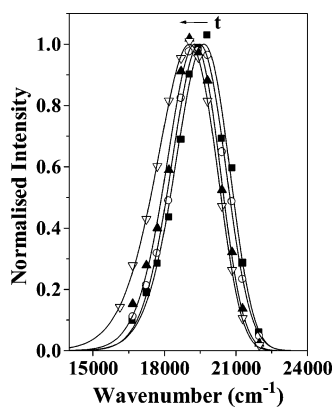


**Figure 7.** Time-resolved emission spectra of C153 bound to 130 mM DIMEB in water at 0 (■), 3 (○), 75 (▲), and 6000 ps (▽).

by two distinct rise constants of 7.8 and 1700 ps (Figure 6). Using the parameters of best fit to the fluorescence decays and the steady-state emission spectrum, the time-resolved emission spectra (TRES) were constructed (Figure 7). To determine the total dynamic Stokes shift for C153 in DIMEB, we used the femtosecond data for short time and the picosecond data for longer times. Using the combined picosecond and femtosecond data, the total Stokes shift for C153 bound to DIMEB is found to be  $600\text{ cm}^{-1}$ .

The solvation dynamics is described by the decay of the solvent correlation function  $C(t)$ , defined as,<sup>23–24</sup>

$$C(t) = \frac{\nu(t) - \nu(\infty)}{\nu(0) - \nu(\infty)} \quad (9)$$

where  $\nu(0)$ ,  $\nu(t)$ , and  $\nu(\infty)$  are the peak frequencies at time 0,  $t$ ,

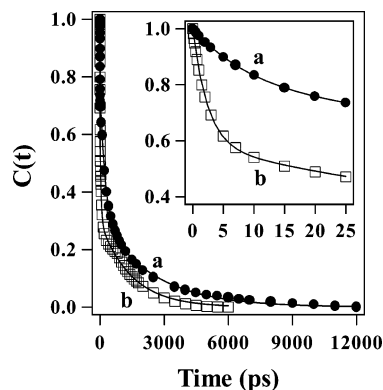


**Figure 8.** Decay of response function  $C(t)$  of C153 bound to (a) 130 mM TRIMEB (●) and (b) 130 mM DIMEB (□) in water. The points denote the actual values of  $C(t)$ , and the solid line denotes the best fit to an exponential decay. Initial parts of the decays of  $C(t)$  are shown in the inset.

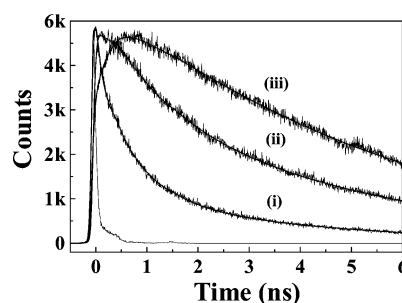


**Figure 9.** Fluorescence decays of C153 in 130 mM TRIMEB in water at (i) 455, (ii) 490, and (iii) 600 nm recorded in picosecond time resolution.

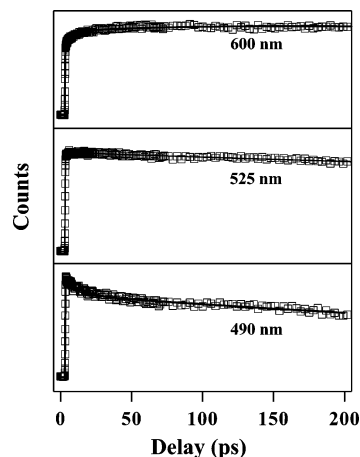


**Figure 10.** Fluorescence decays of C153 in 130 mM TRIMEB in water at (i) 490, (ii) 525, and (iii) 600 nm recorded in femtosecond time resolution.

and  $\infty$ , respectively. The decay of  $C(t)$  is shown in Figure 8, and the decay parameters are summarized in Table 3. The decay of  $C(t)$  for C153 bound to DIMEB is found to be triexponential with time components 2.4 ps (41%), 50 ps (29%), and 1450 ps (30%).

**3.4.3. Picosecond and Femtosecond Result on C153 Bound to TRIMEB.** Figures 9 and 10 respectively describe the wavelength-dependent fluorescence decays of the C153–TRIMEB inclusion complex obtained using a picosecond and a femtosecond setup. The corresponding TRES are given in Figure 11. In this case, the combined result of the picosecond and femtosecond measurements indicates that the decay of  $C(t)$  exhibits three slow components of 10.3 ps (24%), 240 ps (45%),

**TABLE 3: Decay Parameters of  $C(t)$  of C153 in 130 mM DIMEB and TRIMEB**

	C153–DIMEB	C153–TRIMEB		C153–DIMEB	C153–TRIMEB
$a_1^a$	0.41	0.24	$a_3^a$	0.30	0.31
$\tau_1^a$ (ps)	2.4	10.3	$\tau_3^a$ (ps)	1450	2450
$a_2^a$	0.29	0.45	$\Delta\nu^a$ (cm $^{-1}$ )	600	1050
$\tau_2^a$ (ps)	50	240			

<sup>a</sup>  $\pm 10\%$ .

and 2450 ps (31%) (Figure 8, Table 3). The total Stokes shift for C153 bound to TRIMEB is found to be 1050 cm $^{-1}$ .

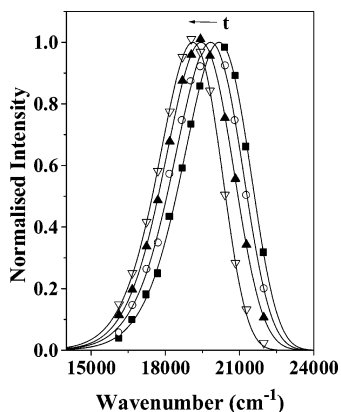


**Figure 11.** Time-resolved emission spectra of C153 bound to 130 mM TRIMEB in water at 0 (■), 50 (○), 500 (▲), and 12000 ps (▽).

#### 4. Discussions

The most important finding of this work is the detection of the slow components of solvation dynamics in the two cyclodextrin (DIMEB and TRIMEB) cavities. It is also interesting to note that while DIMEB displays an ultrafast component of 2.4 ps (41%), in TRIMEB the decay of  $C(t)$  is slower and there is no such ultrafast component. We will now try to find out the possible reasons for these.

There may be several possible sources of the slow component of solvation dynamics. Several groups studied the entry and exit of the probe in the cyclodextrin cavity. It has been demonstrated that this occurs in a 100 ns time scale,<sup>22</sup> which is too slow to explain the components of solvation dynamics in 2.4, 50, and 1450 ps for DIMEB and 10.3, 240, and 2450 ps for TRIMEB. According to a computer simulation, an aromatic molecule makes five jumps in and out of a cyclodextrin cavity in 100 ps.<sup>25</sup> One might argue that the water molecules inside the CD cavity are completely immobilized and solvation dynamics requires an “outward” jump of the probe from the cavity so as to experience solvation by “free” water molecules outside the cavity. Following excitation the highly polar excited probe C153 may move out of the CD cavity to bulk water. If this is the case, at short time the emission spectrum would be broad because of superposition of emission spectra of C153 in CD and bulk water. With an increase in time as C153 diffuses into bulk water, and experiences a uniform environment, the emission spectrum should narrow down. Such a time-dependent decrease in the width of TRES has been reported earlier for self-diffusion of a probe inside a microemulsion.<sup>10a</sup> In the case of DIMEB and TRIMEB there is negligible change in the width ( $\Gamma$ ) of the emission spectra with time. This suggests that the role of self-motion of the probe (C153) out of the CD cavity is minor in the case of DIMEB and TRIMEB.

Another possible source of the slow component may be dynamic exchange of the free and bound water as proposed by Nandi and Bagchi.<sup>8b</sup> In this model, the bound water refers to

the highly immobilized water molecules bound to the cyclodextrin. According to the dynamic exchange model the slow component of the solvation dynamics originates from the interconversion of the bound state to the free state of the water molecules. The magnitude of the slow component of solvent relaxation depends on the energy difference ( $\Delta G^\circ$ ) between the bound and the free state of the water molecules. In the limit of very high  $\Delta G^\circ$ , the slow component of solvation ( $\tau_{\text{slow}}$ ) is given by<sup>8b</sup>

$$\tau_{\text{slow}} \approx k_{\text{bf}}^{-1} \quad (10)$$

where  $k_{\text{bf}}$  is the rate constant for bound-to-free interconversion,

$$k_{\text{bf}} = \left( \frac{k_{\text{B}}T}{h} \right) \exp\left( \frac{-(\Delta G^0 + \Delta G^*)}{RT} \right) \quad (11)$$

where  $\Delta G^*$  is the activation energy for the conversion of free-to-bound water molecules. From eqs 10 and 11 and with use of the solvation times, one may calculate the energy difference ( $\Delta G^\circ$ ) between the bound and free water molecules. However, because of the fact that solvation dynamics is nonexponential even in simple liquids and, in the present case, there are more than one kind of complexes (1:1 and 1:2), straightforward application of these equations (Nandi–Bagchi model) is difficult.

It may be noted that in DIMEB there is a major component (41%) of 2.4 ps which is about 2 times longer than the slowest ( $\sim 1$  ps) component in bulk water. The slight slowing down may be due to structuring of water molecules around the rim of DIMEB. For TRIMEB, the slowest component (10.3 ps, 24%) is about an order slower than the slowest component in bulk water. TRIMEB is totally devoid of hydroxyl groups, while DIMEB has seven secondary hydroxyl groups around the probe. These hydroxyl groups may form strong hydrogen bonds with water molecules, and, hence, there are a lot of water molecules around the probe C153 in DIMEB. In TRIMEB, the methoxy groups are expected to bind weakly to water molecules. Thus there may be fewer water molecules around the probe in C153 in TRIMEB. The slower solvation dynamics and the absence of an ultrafast component in TRIMEB may be ascribed to the nonavailability of a large number of water molecules around the probe C153.

#### 5. Conclusion

This work demonstrates that because of the large binding constant and higher solubility of DIMEB and TRIMEB, almost all of the probe molecules (C153) remain bound to the substituted CDs at a concentration of 130 mM in the form of 1:1 and 1:2 complexes. It is shown that anisotropy decay may be utilized to estimate the dimension of the 1:1 and 1:2 complexes. It is observed that, in the inclusion complexes involving DIMEB, 41% of the total solvation dynamics is very fast (2.4 ps) but the rest of the solvation dynamics is much slower with components 50 and 1450 ps. In comparison to DIMEB, the solvation dynamics in TRIMEB is much slower

with components 10.3, 240, and 2450 ps. The slower solvation dynamics in TRIMEB is attributed to the nonavailability of a large number of water molecules around the methoxy groups of TRIMEB.

**Acknowledgment.** Thanks are due to the Department of Science and Technology, India (Project No. IR/I/CF-01/2002), and the Council of Scientific and Industrial Research (CSIR) for generous research grants. D.R., S.K.M., K.S., and S.G. thank CSIR for awarding fellowships. We thank Professor T. Tahara, Dr. D. Mandal, and Dr. R. Karmakar for many helpful suggestions regarding our femtosecond setup.

## References and Notes

- (1) (a) Szteli, J. *Chem. Rev.* **1998**, *98*, 1743. (b) Saenger, W. In *Inclusion Compounds*; Atwood, J. L., Davies, J. E., MacNicol, D. D., Eds.; Academic: New York, 1984; Vol. 2, p 231. (c) Luzkhov, V.; Aqvist, J. *Chem. Phys. Lett.* **1999**, *302*, 267. (d) Douhal, A. *Chem. Rev.* **2004**, *104*, 1955. (e) Bortulos, P.; Monti, S. *Adv. Photochem.* **1995**, *21*, 1.
- (2) (a) Uekama, K.; Hirayama, F.; Irie, T. *Chem. Rev.* **1998**, *98*, 2045. (b) Khajehpour, M.; Troxler, T.; Nanda, V.; Vanderkooi, J. M. *Proteins* **2004**, *55*, 275. (c) Gaitano, G. G.; Brown, W.; Tardajos, G. *J. Phys. Chem. B* **1997**, *101*, 710.
- (3) (a) Millar, D. P.; Robbins, R. J.; Zewail, A. H. *J. Chem. Phys.* **1982**, *76*, 2080. (b) Wittouck, N. W.; Negri, R. M.; De Schryver, F. C. *J. Am. Chem. Soc.* **1994**, *116*, 10601. (c) Quitevis, E. L.; Marcus, A. H.; Fayer, M. D. *J. Phys. Chem.* **1993**, *97*, 5762. (d) Krishna, M. G. M.; Das, R.; Periasamy, N.; Nityananda, R. *J. Chem. Phys.* **2000**, *112*, 8502. (e) Sen, S.; Sukul, D.; Dutta, P.; Bhattacharyya, K. *J. Phys. Chem. A* **2001**, *105*, 7495.
- (4) (a) Scypinski, S.; Drake, J. M. *J. Phys. Chem.* **1985**, *89*, 2432. (b) Balabai, N.; Linton, B.; Nappaer, A.; Priyadarshi, S.; Sukharevsky, A. P.; Waldeck, D. H. *J. Phys. Chem. B* **1998**, *102*, 9617.
- (5) (a) Fecko, C. J.; Eaves, J. D.; Loparo, J. J.; Tokmakoff, A.; Geissler, P. L. *Science* **2003**, *301*, 1698. (b) Jimenez, R.; Fleming, G. R.; Kumar, P. V.; Maroncelli, M. *Nature* **1994**, *369*, 471. (c) Jarzaba, W.; Walker, G. C.; Johnson, A. E.; Kahlow, M. A.; Barbara, P. F. *J. Phys. Chem.* **1988**, *92*, 7039. (d) Nandi, N.; Roy, S.; Bagchi, B. *J. Chem. Phys.* **1995**, *102*, 1390.
- (6) (a) Nandi, N.; Bhattacharyya, K.; Bagchi, B. *Chem. Rev.* **2000**, *100*, 2013. (b) Pal, S. K.; Zewail, A. H. *Chem. Rev.* **2004**, *104*, 2099. (c) Bhattacharyya, K. *Acc. Chem. Res.* **2003**, *36*, 95. (d) Bhattacharyya, K.; Bagchi, B. *J. Phys. Chem. A* **2000**, *104*, 10603.
- (7) (a) Vajda, S.; Jimenez, R.; Rosenthal, S. J.; Fidler, V.; Fleming, G. R.; Castner, E. W., Jr. *J. Chem. Soc., Faraday Trans.* **1995**, *91*, 867. (b) Nandi, N.; Bagchi, B. *J. Phys. Chem.* **1996**, *100*, 13914. (c) Sen, S.; Sukul, D.; Dutta, P.; Bhattacharyya, K. *J. Phys. Chem. A* **2001**, *105*, 10635.
- (8) (a) Jordanides, X. J.; Lang, M. J.; Song, X.; Fleming, G. R. *J. Phys. Chem. B* **1999**, *103*, 7995. (b) Nandi, N.; Bagchi, B. *J. Phys. Chem. B* **1997**, *101*, 10954. (c) Pal, S. K.; Peon, J.; Zewail, A. H. *Proc. Natl. Acad. Sci. U.S.A.* **2002**, *99*, 1763. (d) Pal, S. K.; Mandal, D.; Sukul, D.; Sen, S.; Bhattacharyya, K. *J. Phys. Chem. B* **2001**, *105*, 1438. (e) Sen, P.; Mukherjee, S.; Dutta, P.; Halder, A.; Mandal, D.; Banerjee, R.; Roy, S.; Bhattacharyya, K. *J. Phys. Chem. B* **2003**, *107*, 14563.
- (9) (a) Hara, K.; Kuwabara, H.; Kajimoto, O. *J. Phys. Chem. A* **2001**, *105*, 7174. (b) Mandal, D.; Sen, S.; Tahara, T.; Bhattacharyya, K. *Chem. Phys. Lett.* **2002**, *359*, 77. (c) Shirota, H.; Tamoto, Y.; Segawa, H. *J. Phys. Chem. A* **2004**, *108*, 3244. (d) Hazra, P.; Chakrabarty, D.; Chakraborty, A.; Sarkar, N. *Biochem. Biophys. Res. Commun.* **2004**, *314*, 543.
- (10) (a) Dutta, P.; Sen, P.; Mukherjee, S.; Halder, A.; Bhattacharyya, K. *J. Phys. Chem. B* **2003**, *107*, 10815. (b) Satoh, T.; Okuno, H.; Tominaga, K.; Bhattacharyya, K. *Chem. Lett.* **2004**, *33*, 1090. (c) Willard, D. M.; Riter, R. E.; Levinger, N. E. *J. Am. Chem. Soc.* **1998**, *120*, 4151. (d) Corbeil, E. M.; Riter, R. E.; Levinger, N. E. *J. Phys. Chem. B* **2004**, *108*, 10777. (e) Pant, D.; Levinger, N. E. *J. Phys. Chem. B* **1999**, *103*, 7846.
- (11) (a) Gearheart, L. A.; Somoza, M. M.; Rivers, W. E.; Murphy, C. J.; Coleman, R. S.; Berg, M. A. *J. Am. Chem. Soc.* **2003**, *125*, 11812. (b) Brauns, E. B.; Madaras, M. L.; Coleman, R. S.; Murphy, C. J.; Berg, M. A. *Phys. Rev. Lett.* **2002**, *88*, 158101-1.
- (12) (a) Scodinu, A.; Reilly, T.; Fourkas, J. T. *J. Phys. Chem. B* **2002**, *106*, 1041. (b) Farrer, R. A.; Fourkas, J. T. *Acc. Chem. Res.* **2003**, *36*, 605. (c) Sen, P.; Mukherjee, S.; Patra, A.; Bhattacharyya, K. *J. Phys. Chem. B* **2005**, *109*, 3319. (d) Baumann, R.; Ferrante, C.; Kneuper, E.; Deeg, F.-W.; Brauchle, C. *J. Phys. Chem. A* **2003**, *107*, 2422.
- (13) (a) Pal, S. K.; Sukul, D.; Mandal, D.; Bhattacharyya, K. *J. Phys. Chem. B* **2000**, *104*, 4529. (b) Sykora, J.; Kapusta, P.; Fidler, V.; Hof, M. *Langmuir* **2002**, *18*, 571. (c) Chattopadhyay, A.; Mukherjee, S. *Langmuir* **1999**, *15*, 2142.
- (14) (a) Frauchiger, L.; Shirota, H.; Uhrich, K. E.; Castner, E. W., Jr. *J. Phys. Chem. B* **2002**, *106*, 7463. (b) Sen, S.; Sukul, D.; Dutta, P.; Bhattacharyya, K. *J. Phys. Chem. B* **2002**, *106*, 3763. (c) Halder, A.; Sen, P.; Das Burman, A.; Bhattacharyya, K. *Langmuir* **2004**, *20*, 653.
- (15) (a) Bandyopadhyay, S.; Chakraborty, S.; Balasubramanian, S.; Bagchi, B. *J. Am. Chem. Soc.* **2005**, *127*, 4071. (b) Marchi, M.; Sterpone, F.; Ceccarelli, M. *J. Am. Chem. Soc.* **2002**, *124*, 6787.
- (16) (a) Pal, S.; Balasubramanian, S.; Bagchi, B. *J. Phys. Chem. B* **2003**, *107*, 5194. (b) Bruce, C. D.; Senapati, S.; Berkowitz, M. L.; Perera, L.; Forbes, M. D. E. *J. Phys. Chem. B* **2002**, *106*, 10902.
- (17) (a) Faeder, J.; Albert, M. V.; Ladanyi, B. M. *Langmuir* **2003**, *19*, 2514. (b) Senapathy, S.; Chandra, S. *J. Phys. Chem. B* **2001**, *105*, 5106. (c) Senapati, S.; Berkowitz, M. L. *J. Chem. Phys.* **2003**, *118*, 1937.
- (18) (a) Thompson, W. H. *J. Chem. Phys.* **2002**, *117*, 6618. (b) Thompson, W. H. *J. Chem. Phys.* **2004**, *120*, 8125. (c) Gomez, J. A.; Thompson, W. H. *J. Phys. Chem. B* **2004**, *108*, 20144. (d) Michael, D.; Benjamin, I. *J. Chem. Phys.* **2001**, *114*, 2817.
- (19) Jones, G., II; Jackson, W. R.; Choi, C.-Y.; Bergmark, W. R. *J. Phys. Chem.* **1985**, *89*, 294.
- (20) (a) O'Connor, D. V.; Phillips, D. *Time Correlated Single Photon Counting*; Academic Press: London, 1984. (b) Kumar, P. V.; Maroncelli, M. *J. Phys. Chem.* **1995**, *99*, 3038. (c) Krolicki, R.; Jarzaba, W.; Mostafavi, M.; Lampre, I. *J. Phys. Chem. A* **2002**, *106*, 1708.
- (21) Hoshino, M.; Imamura, M.; Ikehara, H.; Hamai, Y. *J. Phys. Chem.* **1981**, *85*, 1820.
- (22) Okano, L. T.; Barros, T. C.; Chou, D. T. H.; Bennet, A. J.; Bohne, C. *J. Phys. Chem. B* **2001**, *105*, 2122.
- (23) (a) Maroncelli, M.; Fleming, G. R. *J. Chem. Phys.* **1987**, *86*, 6221. (b) Fee, R. S.; Maroncelli, M. *Chem. Phys.* **1994**, *183*, 235.
- (24) Lakowicz, J. R. *Principles of Fluorescence Spectroscopy*; Kluwer/Plenum: New York, 1999.
- (25) van Helden, S. P.; van Eyck, B. P.; Mark, A.; van Gunsteren, W. F.; Janssen, L. H. M. In *The Sixth International Cyclodextrin Symposium*, Chicago 1992, Abstract; 1992; p L-24.